We are IntechOpen, the world's leading publisher of Open Access books Built by scientists, for scientists

4,800
Open access books available

122,000
International authors and editors

135M
Downloads

Our authors are among the

154
Countries delivered to

TOP 1%
most cited scientists

12.2%
Contributors from top 500 universities

CLARIVATE ANALYTICS BOOK CITATION INDEX INDEXED

WEB OF SCIENCE™

Selection of our books indexed in the Book Citation Index in Web of Science™ Core Collection (BKCI)

Interested in publishing with us?
Contact book.department@intechopen.com

Numbers displayed above are based on latest data collected.
For more information visit www.intechopen.com

27

Optical Spectral Structure and Frequency Coherence

Ning Hua Zhu, Wei Li, Jian Hong Ke, Hong Guang Zhang,
Jiang Wei Man and Jian Guo Liu
Institute of Semiconductors, Chinese Academy of Sciences
P. R. China

1. Introduction

To account for the various phenomena of light, two theories have been proposed: the corpuscular and the undulatory. The former assumes that the light is a stream of corpuscles, namely photons, discrete photons carrying packets of energy and momentum. The undulatory theory, on the other hand, requires that light consists of a series of wave trains (Michelson, 1927). Each wave train is followed by another which has a random change in phase (Mathieu, 1975). A single wave train is made up of monochromatic components, i.e. the wave train is polychromatic. Although wave trains are supposed not to be strictly monochromatic, experimental demonstration is extremely difficult and has not been reported to date (Diitchburn, 1963). In addition, many efforts have been made to measure the laser coherence length which is regarded as the length of the wave train. Among the methods for measuring the coherence length of lasers (Geng et al., 2005; Ryabukho et. al., 2005 ; Wheeler et al., 2003), Michelson interferometer-based method (Ryabukho et al., 2005) is the one widely used in the past. However, these methods suffer from mechanic vibration, thermal and acoustic fluctuations, and beam divergence, and errors in the observation of the spatial coherence are difficult to eliminate. For lightwave from a real laser source, the wave trains are neither identical nor of simple form (Born & Wolf, 1999). Unfortunately, a complete description of other properties, such as linewidth, intensity profile, and frequency spacings among wave trains, has not been explicitly given due to resolution limitations in both measuring techniques and instruments.

Understanding the spectral structure of semiconductor laser is a fundamental issue. The spectral analysis, especially for the fine spectral structure, reveals the important properties of semiconductor laser, such as mode characteristics, atom emission behavior, high-frequency performances, and coherence features. Spectral lines of light are broadened by various processes. For semiconductor lasers, Henry's model (Henry, 1982) can be used to explain linewidth broadening of the laser by two mechanisms: 1) the instantaneous phase change caused by the spontaneous emission results in the linewidth broadening of the light; 2) the instantaneous fluctuations of the field intensity through linewidth enhancement parameter a results in a delayed phase change, which further broadens the linewidth. However, this model also can not describe the properties of wave trains mentioned above distinctly. Indeed, it implies that the spectral linewidth we observed, in fact, results from the

rapid shift of some narrower linewidth elements. This rapid shift derives from the above two fluctuation mechanisms through a series of spontaneous emission events.

In this chapter, we use an interference technique based on the division of frequency to characterize the wave trains of semiconductor lasers, and present a spectral structure model in the frequency-time domain. The assumptions for the model are demonstrated through a series of experiments. It has also been proved that this interference technique has a resolving power of 10^{17} in optical spectral analysis compared to 10^5 of Michelson-interferometer-based methods. At the same time, the powerful resolving ability of this technique enables us to show that the spectral linewidth of the wave train is narrower than 1 mHz. Based on the spectral structure model, a new concept of frequency coherence is proposed, which is different from the conventionally used concepts, such as temporal, spatial and spectral coherence. Moreover, the elimination of the frequency coherence between two lightwaves is also discussed. Frequency coherent lightwaves generation is achieved by a self-injected distributed Bragg reflector (DBR) laser. In addition, monolithically integrated photonic microwave source based the frequency coherent lightwaves generation is experimentally demonstrated.

2. Optical spectral structure model

The commonly used method for spectral analysis has been two-beam or multiple-beam interference. In general, there are two methods to obtain beams from a lightwave source: division of amplitude and division of wave-front (Born & Wolf, 1999). The frequency-division scheme shown in Fig. 2.1(a) is used to measure the linewidth of the wave train. In the following, the spectral linewidth, frequency spacings, and intensity profile among wave trains are investigated through a series of experiments (Zhu et al., 2007).

a. Spectral linewidth and Frequency spacings

Fig. 2.1(a) illustrates the frequency-division scheme, which allows us to perform optical heterodyning at nonzero frequency. This makes it possible to measure the linewidth of wave train with a high-resolution electrical spectrum analyzer instead of observing the fringe visibility.

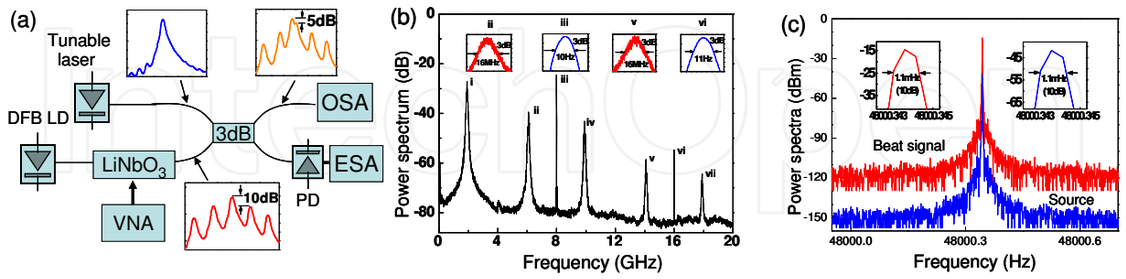

Fig. 2.1. Spectral linewidth analysis of lightwave source and wave trains. (a) Experimental setup. (b) Measured power spectrum of the beat note. Insets show the higher resolution spectra. (c) Measured hyperfine spectrum compared with the power spectrum of the waveform generator

The results (Fig. 2.1(b)) show that the linewidth of the beat note between the lightwaves from different sources is 16 MHz, corresponding to the linewidth of the distributed feedback laser diode (DFB LD). The beat note at the modulation frequency is about 10 Hz, which is

much narrower than the linewidth of the lightwave source. This narrow beat note comes from the interference between the coherence wave trains in the carrier and the sidebands of the intensity modulated lightwave. To precisely estimate the linewidth of the wave trains, a high-resolution spectrum analyzer and a pure electrical source are used. Fig. 2.1(c) shows that the measured 10-dB linewidths of both the beat note and the electrical source are about 1.1 mHz, and no obvious broadening is observed for the beat note. Hence, the linewidth of the wave train should be less than 1 mHz. The above experiment also verifies the assumption that the wave trains emitting simultaneously have random frequency spacings. If this is not the case, the beat note at the modulation frequency cannot be in such a narrow frequency range. From Fig. 2.1(a) and (b), it can be seen that the optical power of the reference signal is 5 dB higher than that of the carrier in the signal channel. But peak ii (beating between the reference signal and the lower sideband) is 15 dB lower than peak iii (beating between carrier and two sidebands). The 17-dB (5+15-3=17) discrepancy is due to the beat note between the wave trains in the carrier and the corresponding wave trains in the two sidebands which are always superposed at the modulation frequency.

b. Intensity profile and duration

The experimental setup shown in Fig. 2.2(a) is used to investigate the interference between lightwaves from the same laser source when a path difference exists. The optical intensity of the reference signal is 15 dB higher than that of the carrier in the signal channel. When the fiber interferometer is made asymmetric by inserting an optical fibre into the reference arm, the beat peak decreases and the noise level increases with path difference. It is because some wave trains in the reference channel, which have length shorter than the path difference, become incoherent with the corresponding wave trains in the sidebands in the signal channel. Interference among these incoherent wave trains produces beat notes whose frequencies spread around the modulation frequency randomly, and leads to an increase in the noise level. This experiment implies that the wave trains have different spatial or temporal lengths.

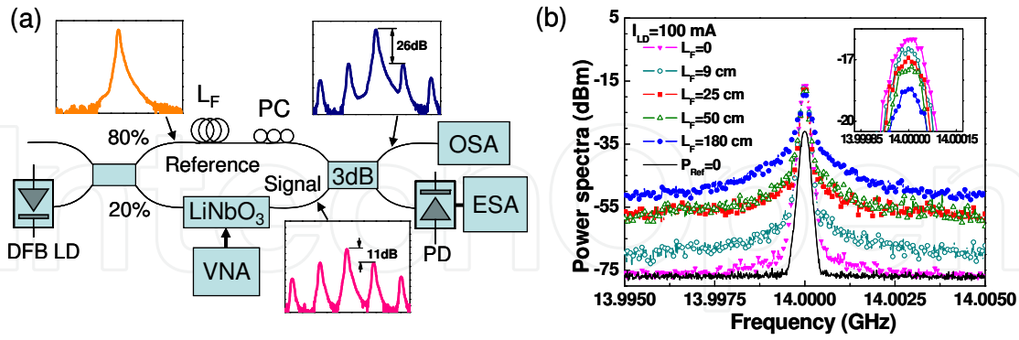

Fig. 2.2. Investigation of interference between lightwaves from one laser source. (a) Experimental setup. PC, polarization controller; LF is the fiber length difference between two arms of the M-Z interferometer. (b) Measured power spectra at various fiber length differences. The curve "P_{ref}=0" indicates the spectrum without reference signal injection. The inset shows the higher resolution spectrum

In order to estimate the length of the wave trains we propose a filtered M-Z interferometer scheme as shown in Fig. 2.3(a). This all-fibre experimental setup is superior to the Michelson interferometer because there is no problem of beam divergence. For lightwave from a real

source, atom emission is irregularly modified by the disturbance from its neighbors, and the duration of wave trains will vary randomly in a certain range. The fluctuation of the beat note is the reflection of the essential pattern of atom emission. The results (Fig. 2.3(b)) show that the beat notes at different bias currents have a dip at the fiber length difference of 2.2 m, and a peak at 4.6 m. Another small peak at 9.2 m can also be observed. The dip and peak values increase with bias current, but the locations change slightly. The conventional ideal models presented in the past literatures (Diitchburn, 1963 ; Born & Wolf, 1999) are unable to explain this phenomenon. If all wave trains are identical and of simple form, the measured beat magnitude will decrease linearly with path difference. Based on the atom emission law (Mandel & Wolf, 1995), we can assume that the rising and decay times are not identical, and before a wave train vanishes it seeds another wave train with the same frequency. Therefore, the probability of occurrence for the two or more joint wave trains with the same frequency is high. Subsequent wave trains may have different frequencies, but the probability is higher for those having closer frequency. When the path difference is half the wave train length, the beat note is at its minimal value. When the path difference is about the wave train length, the beat note reaches its second peak. Therefore, the average length of wave trains is estimated to be about 4.6 m.

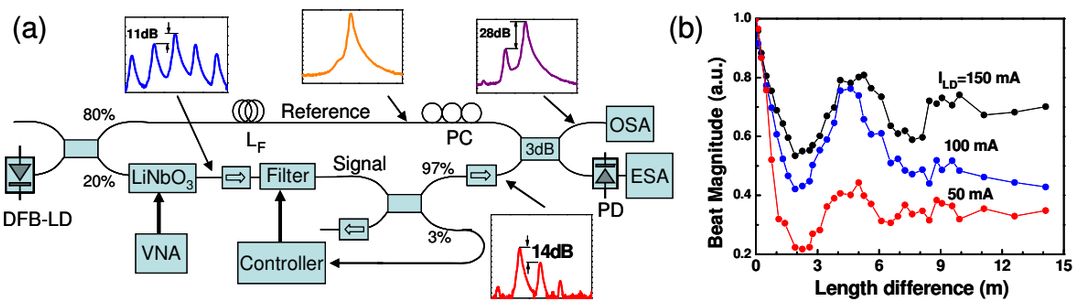

Fig. 2.3. Estimation of coherence length. (a) Experimental setup with the measured optical spectra. A narrow band (2GHz) optical filter is added to the setup (Fig. 2.3(a)) to remove the carrier signal in the signal channel. Three optical isolators are used for the filter to be locked to one of the first-order sidebands. (b) Measured magnitude of the beat notes at different fiber length differences when the DFB laser is biased at 50, 100, and 150 mA, respectively

The resolving power of the Michelson interferometer is limited by the beam divergence. Frequency modulated continuous wave measurement has been used to estimate the coherence length of over 210 km in air using an all-fibre experimental setup (Geng et al., 2005). For the same reason, the interferometer (Fig. 2.3(a)) is stable and can achieve a relatively large path difference without losing resolving power if a zero-dispersion fiber is used as the delay line.

Here we give an alternative method for determining precisely the average coherence length. Fig. 2.4(a) shows the typical setup for measuring the small-signal frequency response, from which the fibre dispersion and the chirp parameter of light emitter can be obtained (Devaux et al., 1993). We found that the setup can also be used to determine the length of the wave trains. In this case, the long optical fiber functions as an "interferometer" and its path difference between the carrier and the sidebands depends on the modulation frequency and fiber dispersion. The optical path difference at the p^{th} peak frequency f_p can be expressed as

$$\Delta L_p = \frac{c}{f_p}\left[p - \frac{1}{2}\,\frac{f_{D2}^2 - 3f_{D1}^2}{f_{D2}^2 - f_{D1}^2}\right], \quad p=0, 1, 2, \ldots \tag{1}$$

where c is the light speed in free space, and f_{D1} and f_{D2} are the first and second dip frequencies. It is interesting to notice that ΔL_p depends only on the peak and dip frequencies, and it is not necessary to determine the physical length of the fiber and its dispersion coefficient. Since large dispersion is desirable, the long fiber can be replaced by dispersion compensation fiber or chirped fiber grating.

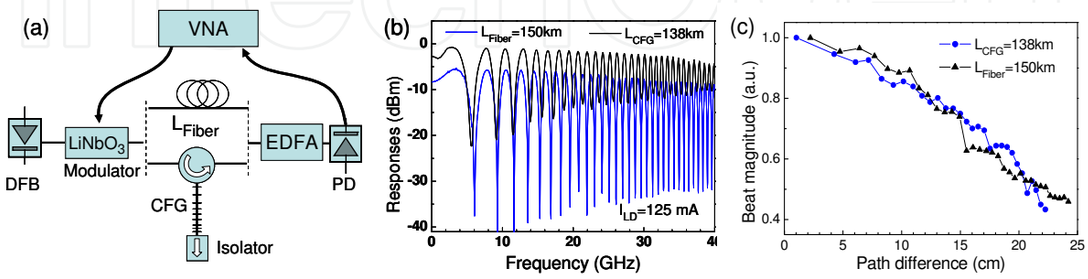

Fig. 2.4. Estimation of coherence length. (a) Experimental setup, in which a long optical fiber or chirped fiber grating (CFG) can be used to achieve a path difference for the lightwaves with different frequencies. (b) Measured frequency responses using a 150-km G652 optical fiber and two chirped fiber gratings for compensating the dispersion of 81+57km G652 fiber when the DFB laser is biased at 125 mA. The measurements are made for 50 times and the curves show the average values. (c) Normalized magnitudes of the corresponding beat note peaks

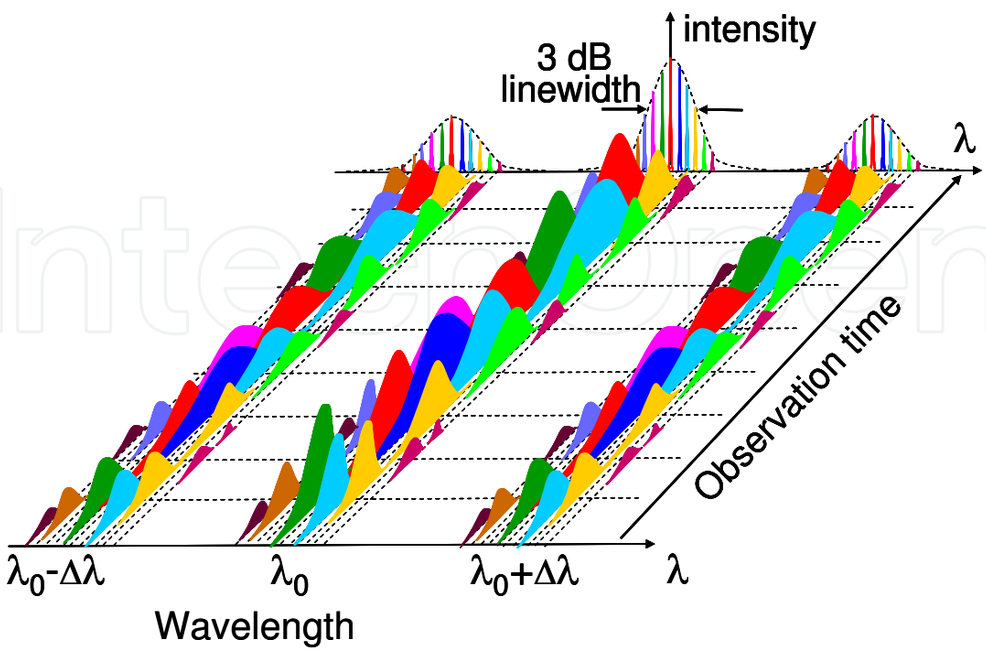

Fig. 2.5. Optical spectral structure model of a semiconductor laser after intensity modulation

The typical frequency responses using a long optical fiber and two chirped fiber gratings are plotted in Fig. 2.4(b), and the corresponding variations of the beat intensity with path difference are shown in Fig. 2.4(c). When the path difference of the "two arms" reaches 20 cm, the average beat note decreases by 3 dB. During the observation time, the changes in modulation frequency and the total fiber length can be neglected since the path difference is less than 25 cm after 150 km propagation. The interference is extremely stable, and the signal to noise ratio can be significantly improved because the wavelength and the polarization of the carrier and the sidebands changes in the same direction, and the two waves propagate in the same medium. Thus, this scheme is simple and suitable for the spectral analysis of a laser with relatively short coherence length.
Based on the above experimental results, we propose an optical spectral structure model as shown in Fig. 2.5, where only the carrier and the first sidebands are shown for simplicity. This model can be summarized as follows: 1) the spectrum of a laser consists of a large number of wave trains. Wave train is not monochromatic and its spectral linewidth is extremely narrow (less than 1 mHz); 2) wave trains are neither identical nor of simple form, and they have variable lengths; 3) wave trains emitting simultaneously will have random frequency spacings, and a wave train can seed another wave train with the same frequency.

3. Frequency coherence

This section presents a new concept of frequency coherence to describe the field correlations between two lightwaves with different frequencies. This concept is different from other well-known coherence concepts, such as temporal coherence, spatial coherence, polarization coherence, quantum coherence, and spectral coherence. Spatial coherence and temporal coherence describe the correlations between beams at different space points and different moments, respectively. Our frequency coherence describes the field correlation between two lightwaves in the frequency-time domain. This model gives a straightforward illustration of optical spectral structure, which is helpful for understanding the spectral structure of semiconductor laser.

3.1 Basic concept of optical coherence

In the broadest sense, optical coherence theory is concerned with the statistical description of the fluctuations of optical fields. Interference is a typical phenomenon that reveals correlation between light beams. Temporal and spatial coherence have been extensively studied in the past come of Michelson and Young's interference experiments, respectively. In a typical interferometer, a beam of lightwave is split into two beams, and the two light beams are recombined together with different delay times. The two beams are perfectly coherent when the lengths of the two paths are identical. For a certain delay difference, the degree of coherence depends on the linewidth and wavelength stability of the light beam. Spatial coherence describes the correlation between signals at different points in space. Temporal coherence describes the correlation between signals observed at different moments. There are other concepts on coherence in accordance with different physical parameters, such as polarization coherence, quantum coherence, and spectral coherence. Spectral correlation, which is not so widely used as temporal and spatial coherence, describes the correlation that exists between the spectral components at a given frequency in the light oscillations at two points in a stationary optical field (Mandel & Wolf, 1976).

3.2 Description in three-dimensional space

The coherence properties of two beams should be described in three-dimensional spaces. Take coherence in space-time domain for example, the three dimensions are distance, time delay, and amplitude. The complex degree of coherence is traditionally used to characterize correlations in stationary fields. It is defined as normalized cross-correlation function of the optical fields at two points. In the following, we briefly introduce the theory of the complex degree of coherence in space-time domain (Mandel & Wolf, 1965).

Suppose that $V(r_1, t)$ and $V(r_2, t)$ are the analytic signal representations of the light oscillations at two points with position vectors r_1 and r_2, the complex degree of coherence can be expressed as

$$\gamma(r_1, r_2, \tau) = \Gamma(r_1, r_2, \tau) / [I(r_1)I(r_2)]^{1/2} \tag{2}$$

where $\Gamma(r_1,r_2,\tau)=<V^*(r_1,t)V(r_2,t+\tau)>$ is the mutual coherence of the light, and $I(r) =\Gamma(r,r,0)$ is the average intensity of the light. For all possible values, $0\leq\gamma(r_1,r_2,\tau)\leq 1$.

If the light is quasimonochromatic, the visibility of fringes at position $P(r)$ on the interference screen is

$$\upsilon(r) = \frac{I_{max}(r) - I_{min}(r)}{I_{max}(r) + I_{min}(r)} = \left|\gamma(r_1, r_2, \tau_{12})\right| \tag{3}$$

which means that $|\gamma|$ is a measure of the sharpness of the interference fringes. The complex degree of spectral coherence in the frequency-time domain (Mandel & Wolf, 1976) is given by

$$\mu(r_1, r_2, \nu) = W(r_1, r_2, \nu) / [W(r_1, r_1, \nu)W(r_2, r_2, \nu)]^{1/2} \tag{4}$$

Where $W(r_1,r_2,\upsilon)$ is the cross-spectral density function (also known as the cross power spectrum) of the two optical fields. Therefore, the coherence properties in the space-time domain depend on position and on the delay time, and the coherence properties in the space-frequency domain depend on position and on the frequency of the light.

3.3 Concept of frequency coherence

It is desirable to give general description of the field correlations between two lightwaves with different frequencies, and to investigate the related phenomena and their applications. Optical heterodyne technique using two lightwaves with different wavelengths has been widely used to generate microwave and millimeter waves. The spectral characteristics and correlations of the two lightwaves are critical in obtaining a stable and narrow-linewidth microwave signal. Referring to the concept of spatial and temporal coherence in the space-time domain and the spectral coherence in the space-frequency domain, we introduce a new concept of frequency coherence in the frequency-time domain, which describes the field correlation between two lightwaves with different frequencies at a given moment.

Given that two arbitrary beams a and b overlapped in wavelength, the optical fields at optical frequencies ω_1 and ω_2 can be expressed as

$$E_1(\omega_1, t) = [E_A f_a(\omega_1, t)e^{-j\varphi_a} + E_B f_b(\omega_1, t)e^{-j\varphi_b}]e^{-j\omega_1 t} \tag{5}$$

$$E_2(\omega_2,t)=[E_A f_a(\omega_2,t)e^{-j\varphi_a}+E_B f_b(\omega_2,t)e^{-j\varphi_b}]e^{-j\omega_2 t} \tag{6}$$

E_A and E_B are the maximal optical fields of beams *a* and *b,* respectively. $f_a(\omega,t)$ and $f_b(\omega,t)$ are the normalized power spectrum profiles and meet

$$\int_0^{+\infty} f_x^2(\omega,t)d\omega=1, \qquad x=a,\ b \tag{7}$$

The photocurrent could be written as

$$\begin{aligned} i(t)\propto{}& \frac{1}{2}E_A^2 f_a^2(\omega_1,t)+\frac{1}{2}E_B^2 f_b^2(\omega_1,t)+\cos\phi E_A E_B f_a(\omega_1,t)f_b(\omega_1,t)\cos\Delta\varphi \\ &+\frac{1}{2}E_A^2 f_a^2(\omega_2,t)+\frac{1}{2}E_B^2 f_b^2(\omega_2,t)+\cos\phi E_A E_B f_a(\omega_2,t)f_b(\omega_2,t)\cos\Delta\varphi \\ &+F(\omega_m)E_A^2 f_a(\omega_1,t)f_a(\omega_2,t)\cos(\omega_m t)+F(\omega_m)E_B^2 f_b(\omega_1,t)f_b(\omega_2,t)\cos(\omega_m t) \\ &+\cos\phi F(\omega_m)E_A E_B f_a(\omega_1,t)f_b(\omega_2,t)\cos(\omega_m t+\Delta\varphi) \\ &+\cos\phi F(\omega_m)E_A E_B f_b(\omega_1,t)f_a(\omega_2,t)\cos(\omega_m t-\Delta\varphi) \end{aligned} \tag{8}$$

where ϕ is the angle between the polarization directions of the two beams, $F(\omega_b)$ is the frequency response coefficient of the photodetector, and $\Delta\varphi=\varphi_a-\varphi_b$ is the phase difference between the two beams. The first six terms in (8) represent the DC beat notes. The 7th and 8th terms indicate homodyne signals. Intensity noise exists at all frequencies simultaneously for wide spectral optical source, and a simple method for the calibration of wide bandwidth photoreceiver has been established (Eichen & Silletti, 1987). The 9th and 10th terms indicate heterodyne signals. Collecting all the optical current components at frequency ω_m from the beat notes of the two beams, we have

$$\begin{aligned} i_{\omega_m}(t)\propto{}& F(\omega_m)E_A^2\cos(\omega_m t)\int_0^{\infty} f_a(\omega_1,t)f_a(\omega_2,t)d\omega_1 \\ &+F(\omega_m)E_B^2\cos(\omega_m t)\int_0^{\infty} f_b(\omega_1,t)f_b(\omega_2,t)d\omega_1 \\ &+\cos\phi F(\omega_m)E_A E_B\cos(\omega_m t+\Delta\varphi)\int_0^{\infty} f_a(\omega_1,t)f_b(\omega_2,t)d\omega_1 \\ &+\cos\phi F(\omega_m)E_A E_B\cos(\omega_m t-\Delta\varphi)\int_0^{\infty} f_b(\omega_1,t)f_a(\omega_2,t)d\omega_1 \end{aligned} \tag{9}$$

When two beams do not overlap, i.e., $f_a(\omega_2,t)=0$, and $f_b(\omega_1,t)=0$, (9) reduces to

$$i_{\omega_m}(t)\propto\cos\phi F(\omega_m)E_A E_B\cos(\omega_m t+\Delta\varphi)\int_0^{\infty} f_a(\omega_1,t)f_b(\omega_2,t)d\omega_1 \tag{10}$$

When the light beams are optical carrier and the sidebands produced by optical intensity modulation, ω_m becomes the modulation frequency. The optical spectral distribution in the frequency-time domain is shown in Fig. 2.5, and only the carrier and the first sidebands are shown for simplicity. Based on the atom emission law and the time response of ultrafast

photonic crystal laser (Yariv, 1997), we can assume that the rising and decay times are not identical. From our understanding of optical spectral distribution, the spectrum of a laser consists of a large number of wave trains. It has been shown that the spectral linewidth of wave trains is narrower than 1 mHz, and the linewidth of DFB laser used is ~ 16 MHz. Also, the simultaneous emitted wave trains have random frequency spacings (Zhu et al., 2007). Therefore, the probability of occurrence of two wave trains from the same lightwave source with a frequency spacing $\omega_m=\omega_2-\omega_1$ is rather low. Thus, we can assume that

$$\int_0^{+\infty} f_x(\omega,t) f_x(\omega+\omega_m,t)d\omega << 1, \qquad \omega_m \neq 0 \tag{11}$$

From the definition of the complex degree of coherence in the space-time and space-frequency domains, the degree of frequency coherence of two beams in the frequency-time domain can be expressed as

$$\gamma(\omega_1,\omega_2,t) = \int_0^{+\infty} f_a(\omega_1,t) f_b(\omega_2,t)d\omega, \tag{12}$$

According to the definition of the power spectrum profile, $0 \leq |\gamma(\omega_1,\omega_2,t)| \leq 1$ for all possible values of γ.

The wave trains in the carrier and the corresponding wave trains in the sidebands appear simultaneously, and their frequency intervals exactly equal the modulation frequency. Since the carrier and the sidebands have identical intensity profile, polarization and phase, i. e., $f_b(\omega_2,t)=f_b(\omega_1+\omega_m,t)=f_a(\omega_1,t)$, and considering the optical spectrum properties indicated by (7) and (11), we have $\gamma(\omega_1,\omega_2,t)=1$. Thus, (9) can be approximated as

$$i_{\omega_m}(t) \propto F(\omega_m) E_A E_B \cos(\omega_m t + \Delta\varphi) \tag{13}$$

It means that the linewidth of the beat note at the modulation frequency is independent of the optical spectral profile of the beams. In this case, the beat note at the modulation frequency is much stronger than the beat notes at other frequencies which become random noise. The carrier and its sidebands produced by intensity modulation are perfectly coherent if there is no time delay. As the path difference increases the beat note at the modulation frequency will decrease and the noise level will increase (Zhu et al., 2007). The carrier and the sidebands may then become partially coherent.

It can be concluded that for the coherent beams the maximum intensity of the mixed beams may exceed the sum of the intensities of the beams (Born & Wolf, 1999), and the beat note between the two beams would have a linewidth much narrower than the sum of the beam linewidths.

4. Experimental analysis of frequency coherence properties

In the above sections, we have presented the new hyperfine spectral structure of semiconductor lasers and the theory of frequency coherence. In this section, frequency coherence properties of different optical lightwaves are experimentally investigated using optical heterodyne technique. The results indicate that the optical carrier and its intensity

modulated sidebands are perfectly coherent and the longitudinal modes of an FP laser are partially coherent (Zhu et al., 2009).

4.1 Modulated optical spectrum: perfectly coherent

For the beams which are coherent, the maximum intensity of the mixed beams may exceed the sum of the intensities of the beams, and the linewidth of the beat note between the two beams would be much narrower than the sum of the beam linewidths. These discrepancies in intensity and linewidth are the key features in describing the coherence properties of lightwaves. The following experiments were designed to analyze the optical and electrical spectra of the beams and the corresponding beat notes.

Fig. 2.6 is the measurement setup. In the first experiment, five lightwave sources, which have different spectral widths, are used, i.e., an amplified spontaneous emission (ASE) lightwave source (an erbium-doped fiber amplifier without optical input signal), the same ASE source together with a 28GHz optical filter and a 5GHz optical filter, an DFB laser with a 16 MHz linewidth, and a tunable laser with a linewidth narrower than 100 kHz. These lightwave sources are all modulated by a 15-GHz signal from a vector network analyzer (VNA) through a $LiNbO_3$ modulator with a bandwidth of 40-GHz. An optical fiber coupler is used to split the output into two waves, and the optical spectrum is measured by an optical spectrum analyzer, and a electrical spectrum analyzer (ESA) and a high-speed photodetector is used to measure the power spectrum. The spectrum is recorded using the "Max Hold" function of the ESA for several seconds. The peak power of the beat note is kept the same for different lightwave sources.

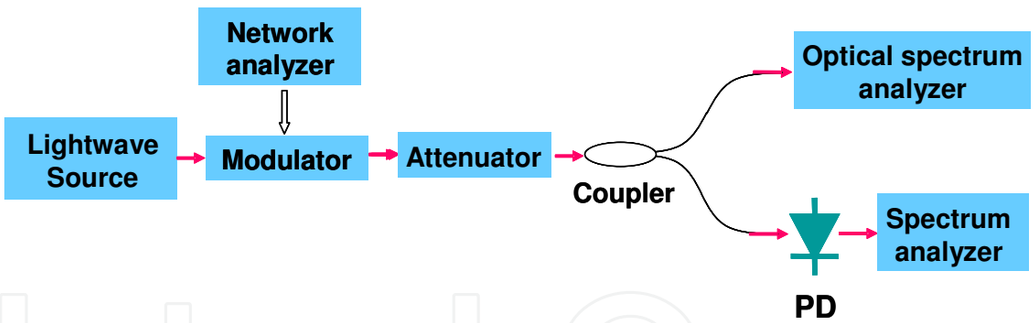

Fig. 2.6. Experiment setup for testing the coherence properties of modulated optical spectrum

Fig. 2.7 shows the measured optical spectra and the corresponding power spectra. For different lightwave sources whose spectrum widths vary from 100 kHz to 5 THz, the measured power spectra are almost identical, and the 6-dB linewidths of the beat notes are about 154 kHz, which depends on the parameters of the instruments, such as the frequency span and the resolution bandwidth of the spectrum analyzer. In the next experiment it will be shown that the beat note between the carrier and the sidebands is extremely narrow.

In the second experiment the measurement setup is the same, except a tunable laser is connected to the other input port of the coupler and acted as a reference lightwave source, and its wavelength is 2 GHz lower than the central wavelength of a DFB laser which is the lightwave source. The modulation frequency is set to be 8 GHz.

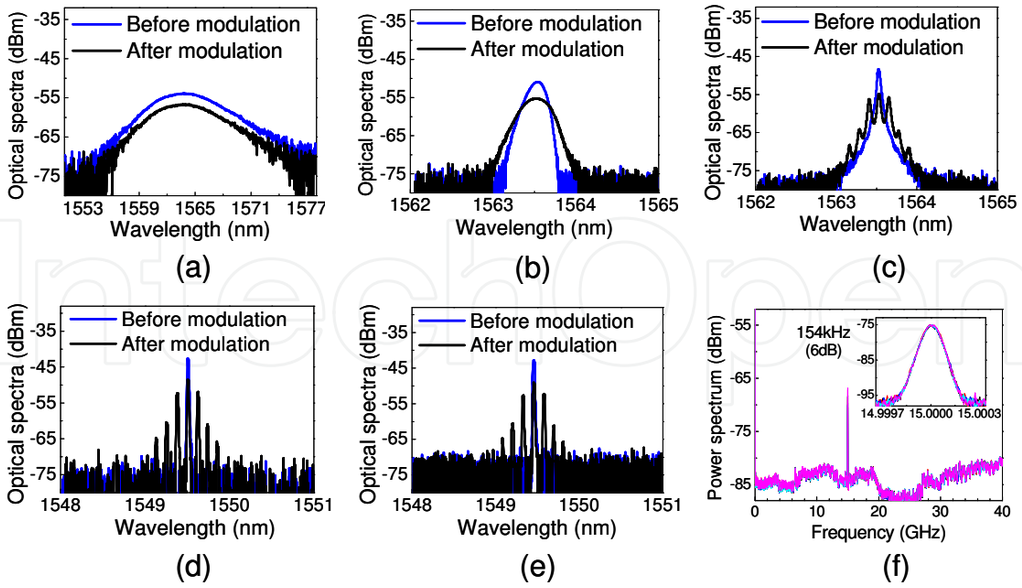

Fig. 2.7. Measured optical spectra (a-e) and the corresponding power spectra (f)

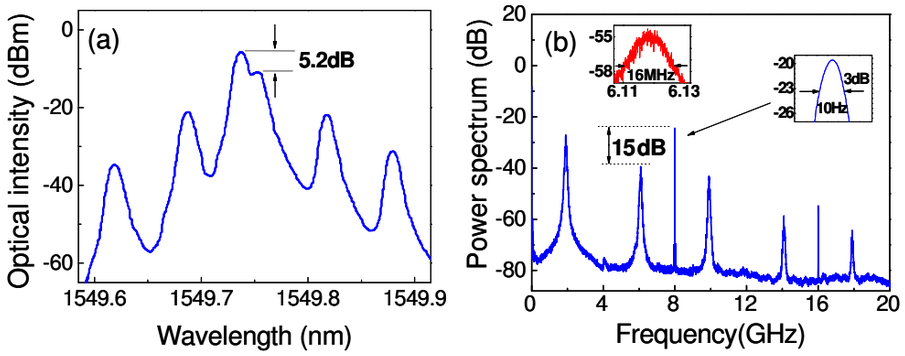

Fig. 2.8. Measured optical and electrical spectra, when the lightwave sources used was a DFB laser, the reference tunable lightwave was from a tunable laser, and the modulation frequency was 8GHz. The inset shows the higher resolution spectrum at the modulation frequency

The optical and electrical spectra are shown in Fig. 2.8. The signal at 6.12 GHz denotes the beat note between the first left sideband and the reference signal. The linewidth of the beat note is 16 MHz and can be considered as the linewidth of the DFB laser since the linewidth of the tunable laser is much narrower, which is less than 100 kHz. The beat note at 8GHz is between the two first sidebands and the carrier. Its linewidth is only 10 Hz.

From Fig. 2.8 it shows that the optical power of the reference signal is 5.2dB higher than that of the carrier of the DFB laser. However, the beat note (at 6GHz) between the carrier and the reference signal is 15dB lower than that of the beat note at 8 GHz. There is a discrepancy of 17.2-dB (15+5.2 - 3=17.2), assuming that the intensities of the two sidebands are equal and the photodetector has the same frequency responses at 6 and 8 GHz.

The experiments above show that the beat note between the carrier and the sidebands is extremely narrow, which is about 10 Hz, and its intensity is 17.2 dB higher than that of the

beat notes between the lightwaves emitted from different lightwave sources. Therefore, the carrier and its sidebands are perfectly coherent.

4.2 Longitudinal modes of FP laser: partially coherent

The mode spacing of a FP laser usually exceeds 100GHz. Thus, the conventional optical heterodyne technique can not be directly used to investigate the frequency coherence properties of an FP laser. To overcome this problem, a measurement setup similar to that shown in Fig. 2.6 is used. The lightwave source is a FP laser diode. After modulation, the high-order sidebands of the adjacent FP modes become close and fall into the operation frequency range of the ESA. An Erbium-doped optical fiber amplifier (EDFA) is used to raise the optical power after intensity modulation. Fig. 2.9(a) shows the measured optical spectra before and after intensity modulation at 30GHz. From this figure it can be seen that the frequency difference between the higher second sideband of FP mode 01 and the lower second sideband of FP mode 02 is about 18 GHz, whose 6-dB linewidth of the beat note is about 7.1 MHz.

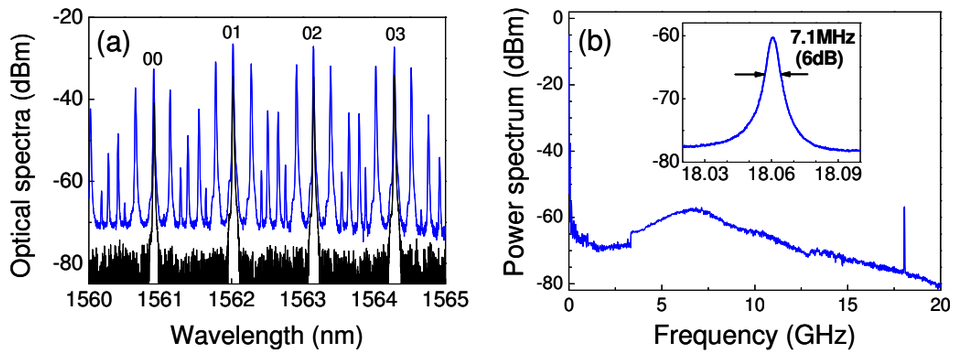

Fig. 2.9. (a) Measured optical spectra of a Fabry-Perot laser before (solid line) and after (dashed line) modulation, where the modulation frequency is 30 GHz. (b) Corresponding spectra, where inset shows the higher resolution spectrum

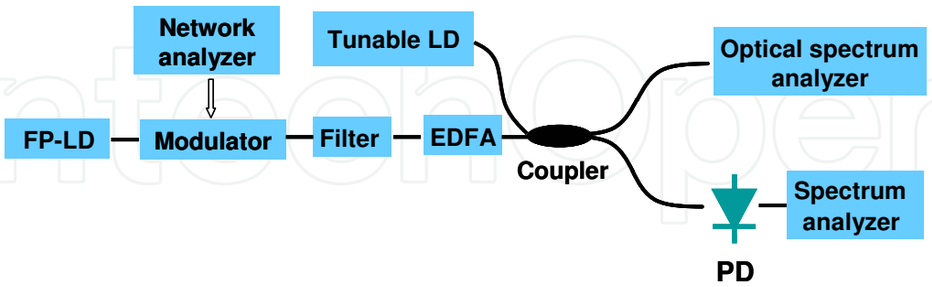

Fig. 2.10. Experiment setup for analysing the frequency coherence properties of longitudinal modes of an FP laser using an optical filter

Another experiment is implemented as shown in Fig. 2.10. A tunable laser is the reference lightwave source, and its wavelength is between the lower second sideband of FP mode 02 and the higher second sideband of FP mode 01. Other optical modes are removed by a 28-GHz bandpass optical filter, and only the shifted second sidebands of FP modes 01 and 02 are considered.

As shown in Fig. 2.11(b), the 6-dB linewidth of the beat note (18.06 GHz) between the second sidebands of FP modes 01 and 02 is about 7.2 MHz. The spectral widths of the beat notes (8.3 and 9.76 GHz) between the reference lightwave and the shifted second sidebands of FP modes 01 and 02 are about 130 MHz. From Fig. 2.11(a) one can see that the optical power of the reference signal is 5dB higher than that of the higher second sideband of FP mode 01. However, the beat note between the lower second sideband of FP mode 02 and the reference signal is 7 dB lower than the beat note between the second sidebands of the FP modes 01 and 02. A discrepancy of 12dB exits. The above results indicate that the FP modes of the laser are coherent. However, the FP modes are not perfectly coherent, if not, the linewidth of the beat note would be extremely narrow. The linewidth of the beat note between the two second sidebands of the FP modes is about 7.2 MHz. This means that the longitudinal modes of the FP laser are partially coherent.

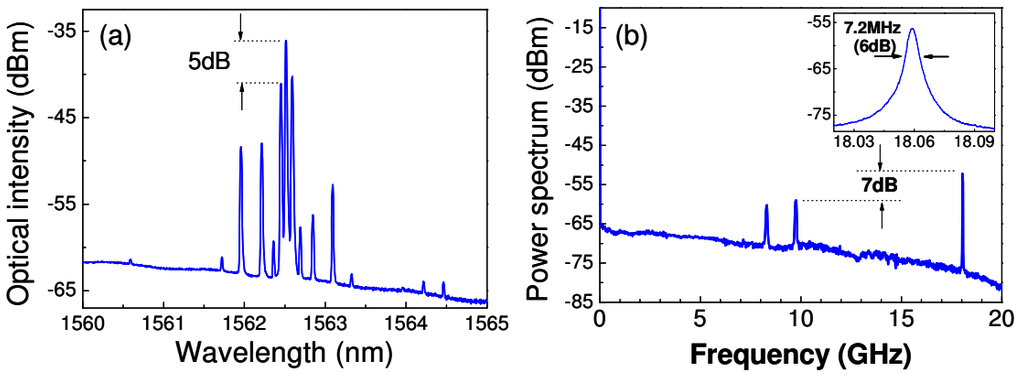

Fig. 2.11. (a) Measured optical spectra when the FP laser is modulated at 30GHz, an optical filter is used. (b) Corresponding spectra, where inset shows the higher resolution spectrum

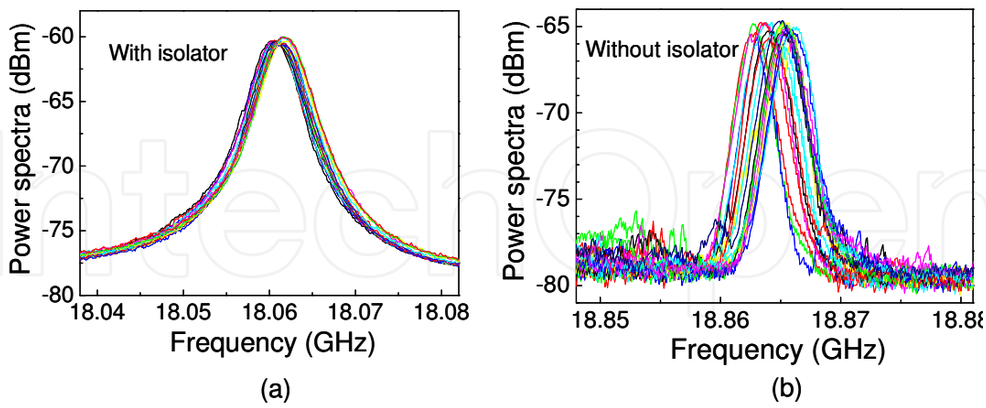

Fig. 2.12. Higher resolution spectra of the laser with (a) and without (b) optical isolator measured for 20 times

The higher resolution spectrum of the optical beat note is measured for 20 times and is shown in Fig. 2.12(a), from which it can be seen that the measured beat note is quite stable. If optical filter is not used, beating may occur between the second sidebands of all neighbouring FP modes. However, from Fig. 2.11(b) and 2.9(b) one can conclude that the

mode spacings and the linewidths of all the adjacent FP modes are almost identical. This coincides with the statement that the modes of FP laser are locked by mutual injection (Sato et al., 2001). However, FP modes are only partially coherent, because the mode locking is based on four-wave mixing, and all modes originate from at least two modes.

Similar experiments are carried out using a FP laser without an optical isolator. The threshold current of the laser is about 10 mA and the bias current is 60 mA. The modulation frequency is 40 GHz. The results are given in Fig. 2.12(b), 2.13, and 2.14.

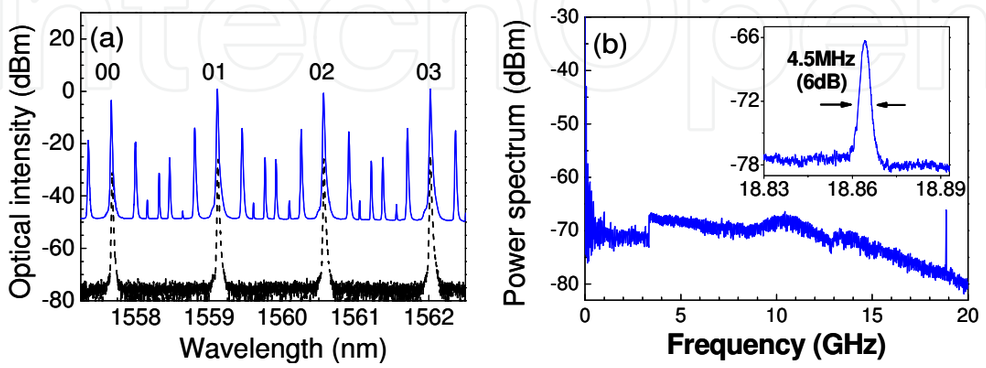

Fig. 2.13. (a) Measured optical spectra when the FP laser without an optical isolator is modulated at 30GHz. (b) Corresponding spectra, where inset shows the higher resolution spectrum

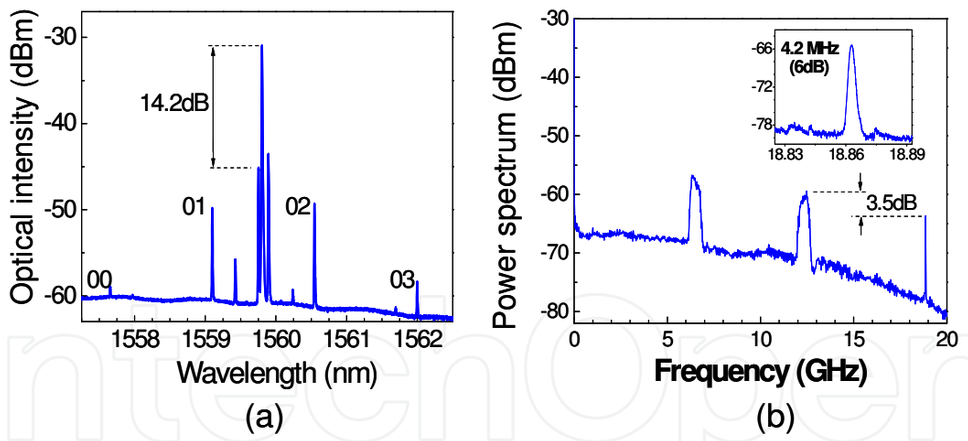

Fig. 2.14. (a) Measured optical spectra when the FP laser without an optical isolator is modulated at 30GHz, an optical filter is used. (b) Corresponding spectra, where inset shows the higher resolution spectrum

Normally the optical wavelengths of the FP laser may be affected by the ambient temperature and bias current. It has been shown that when the chip temperature varies by 1°C the FP modes of the laser will change by 0.1 nm, corresponding to a frequency change of 12.5GHz at 1.55μm (Zhu et al., 2006). Although a Peltier cooler can be used to control the temperature, it is impossible to maintain the chip temperature within 0.0001°C. From Fig. 2.14 one can see that the FP modes shift is about 610 MHz. However, from Fig. 2.12(b) it can be observed that the changes of the FP mode spacing are within 4 MHz. This clearly shows

that the longitudinal mode spacing of the FP laser is relatively fixed, although the wavelengths of the FP modes change with temperature. Therefore, the beat note between the shifted second sidebands is much more stable.
Comparing Fig. 2.12(a) and 2.12(b) it follows that the wavelength of FP laser becomes more stable when an optical isolator is used. Wavelength stability plays an important role in the generation of a stable and narrow-linewidth microwave signal.
From the measured optical and electrical spectra shown in Fig. 2.14, it can be seen that the optical power of the reference signal is 14.2dB higher than that of the higher second sideband of FP mode 01. The beat note between the reference signal and the lower second sideband of FP mode 02 is only 3.5 dB higher than the one between the higher second sideband of FP mode 01 and the lower second sideband of FP mode 02. This discrepancy (10.7dB) and 4.5 MHz linewidth of the beat note between the two sidebands also indicate that the FP modes of the FP laser are partially coherent.

5. Elimination of frequency coherence

In the previous sections, we have theoretically and experimentally demonstrated the concept of frequency coherence. The degree of frequency conherence mainly depends on the spectral characteristics and correlations of the two lightwaves. Although two lightwaves with highly frequency coherence are desirable for generating pure microwave or millimeter wave signals, it is also needed to eliminate the frequency coherence of two lightwaves in some cases, for example, the linewidth measurement of the lasers. In this section, the elimination of the frequency coherence of two lightwaves is investigated experimentally and the phenomena observed in the experiments are explained using the three-dimension optical spectral structure model.

5.1 Three-dimension model of optical spectrum

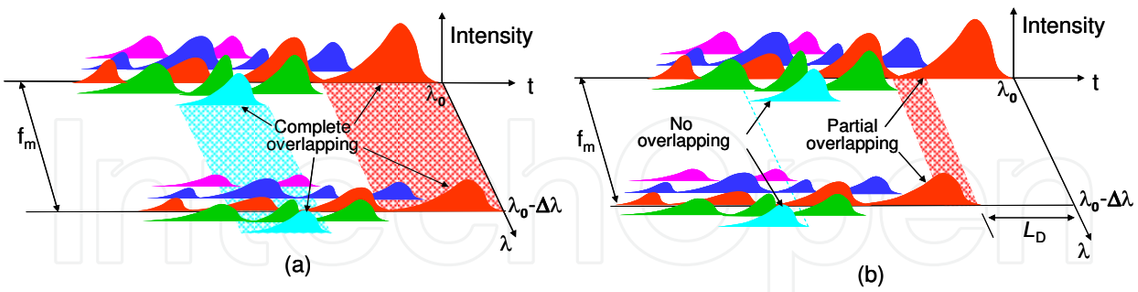

Fig. 2.15. Configuration of optical spectral structure in frequency-time domain after intensity modulation (a) without and (b) with the time delay

Based on optical spectral structure in the frequency-time domain, the spectrum of the light beam consists of a large mount of wave trains around the center wavelength, which have distinct features just as the followings (Zhu et al., 2007).

a. In the frequency domain, it is not strictly monochromatic and the spectral linewidth is much narrower than 1 mHz, corresponding to a wavelength range of 10^{-23} m at 1.55 μm.
b. The wave trains are emitted simultaneously with random frequency spacings. A wave train is able to seed another wave train with the same frequency, and the probability of

occurrence of two or more joint wave trains with the same frequency is rather high. The subsequent wave trains may be with different frequencies, but the probability is much lower.

c. In the time domain, the spatial and temporal intensity profiles of wave trains are neither identical nor of simple form. The length of wave trains has a large variable range. The intensity profile and average duration mainly depend on the laser structure, the bias condition and the optical cavity.

When a light beam is modulated, any wave train in the carrier and the corresponding wave train in the sidebands may appear simultaneously with perfect frequency coherence, and their frequency interval is exactly identical to the modulation frequency. Fig. 2.15 gives the optical spectral structure of the carrier and only one first sideband in the time-frequency domain for simplicity. All the beat notes between wave train pairs in the sideband and carrier are always superposed at the modulation frequency. The beat note at the modulation frequency is much stronger than beat notes at other frequencies, which will become random noise originated from the vicinity of the center wavelength.

If there is a time delay between these two beams, from the optical spectral structure shown in Fig. 2.15, one can see that the corresponding wave trains in carrier and sidebands having coherence lengths longer than the delay time are partially overlapping in time domain. That means these trains are partially frequency coherent, and only part of the beat notes between these wave train pairs are superposed at the modulation frequency. For the wave trains with lengths shorter than the delay time, there is no overlapping in the time domain. The corresponding wave trains in the carrier and sidebands have no coherence and do not beat. If the delay time between sidebands and the carrier is long enough and longer than all wave trains, the two beams become completely incoherent. In this case the measured linewidth of beat note is so called spectral linewidth of light beams.

5.2 Dependence of frequency coherence on delay time

Referring to the Wiener–Khinchin theory (Richter et al., 1986), the optical spectral structure consists of incoherent and coherent parts. We will give the formulation description (Zhu et al. 2010). If the delay time between sideband and the carrier is τ_0, the total optical field can be expressed as:

$$E(t) = E_0 \exp[j(\omega_0 t + \varphi(t))] + \beta E_0 \exp\{j[(\omega_0 + \omega_m)(t+\tau_0) + \varphi(t+\tau_0)]\} \tag{14}$$

where E_0 is the amplitude of optical field, β is a real factor accounting for the amplitude ratio between two fields, ω_0 is the angular frequency of laser beam, ω_m is the modulation frequency, the phase section$\varphi(t+\tau_0)$ and $\varphi(t)$ introduce the phase jitter which is assumed to be a Gaussian distribution. After the necessary formula derivation, the power spectrum $S(\omega)$ can be expressed as:

$$S(\omega) = f_\delta \delta(\omega - \omega_m) + f_L \frac{1}{1 + \left[(\omega - \omega_m)/S_0\right]^2}\ , \tag{15a}$$

where

$$f_\delta = 2\beta^2 E_0^{\,4} \exp(-S_0 \tau_0)\ , \tag{15b}$$

$$f_L = 4\beta^2 E_0^4 \left\{ 1 - \exp(-S_0\tau_0) \left[\cos((\omega - \omega_m)\tau_0) + \frac{S_0}{\omega - \omega_{\mathrm{m}}} \sin((\omega - \omega_{\mathrm{m}})\tau_0) \right] \right\}. \quad (15c)$$

Here only the white noise S_0 originated from atom spontaneous radiation is included. In (15a), the first term is a δ function at modulation frequency, and is the beat note between the coherent wave trains of light beams when the average coherence length is longer than the delay length. It can be concluded that its intensity will decrease with the increase of the delay time. The second term is the beat note between incoherent wave trains which is broadened by the phase random noise. It has a quasi-Lorentzian profile with a weight factor f_L located at the modulation frequency. From (15c) it can be seen that the amplitude of quasi-Lorentzian profile will be proportional with the delay time.

Actually, when the delay fiber is long enough, both the white noise and the $1/f$ noise component are included, and the $1/f$ noise component gives a similar Gaussian profile. In this case, the two light beams will become incoherent and the δ-peak disappears. The power spectrum will become a Voigt lineshape, which is the convolution of the Gaussian profile and Lorentzian profile. The disappearance of the δ-peak can be regarded as the criterion of coherence elimination and the lineshape broadening at the moment can be used as the optical linewidth.

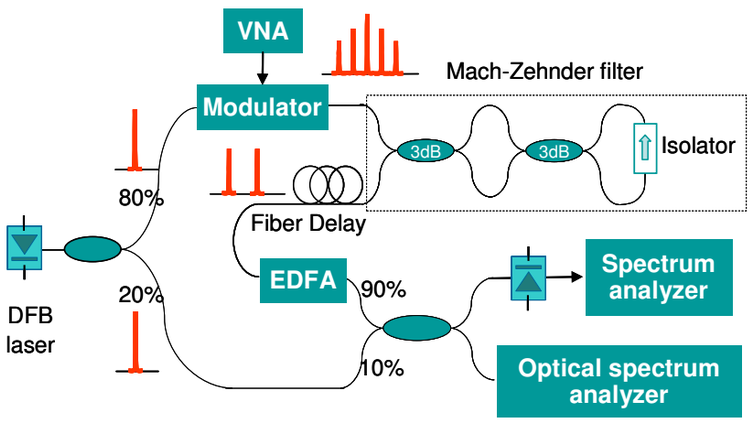

Fig. 2.16. Measurement scheme for lineshape analysis using delayed optical self-heterodyne method

Up to date, lots of methods for analyzing lineshape and linewidth have been established in the past two decades (Chan, 2007; Dawson et al., 1992; Ludvigsen et al., 1998; Richter et al., 1986; Signoret et al., 2001; Signoret et al., 2004; Zhu et al., 2010). The method widely used for analyzing lineshape is delayed self-heterodyne technique. The frequency fluctuations or optical phase of the laser source under test can be converted into intensity variations by an asymmetric Mach-Zehnder type interferometer. Enough fiber delay, which is longer than coherence length, can make no overlapping in time domain between the carrier and sideband, and the frequency coherence between them can be eliminated. Fig. 2.16 illustrates the measurement setup for carrying out the lineshape analysis of beat note between the optical carrier and shifted sidebands based on delayed optical heterodyning in the experiment. A VNA and a $LiNbO_3$ modulator were used to modulate the light beams from the DFB laser and a Mach-Zehnder filter was used to separate the sidebands from the modulated lightwaves.

It has been shown that no matter what optical sources are used, the beat note between first sidebands and the carrier has an extremely narrow linewidth if there is no time delay between them (Zhu et al., 2009). With the increase of the delay line, the coherence between the carrier and the delayed first sidebands will be reduced. Fig. 2.17 shows the measured power spectra of the DFB laser using different delay lines. The power ratios between the δ-peak and the Lorentzian component with different delay lengths are summarized in Table I. It can be seen that the δ-peak decreases and the amplitude of the quasi-Lorentzian profile originated from the noise increases with the increased delay line. When the delay fiber is over 10 km, δ-peak disappears and the coherence between the carrier in the reference channel and the delayed first sidebands has been eliminated completely.

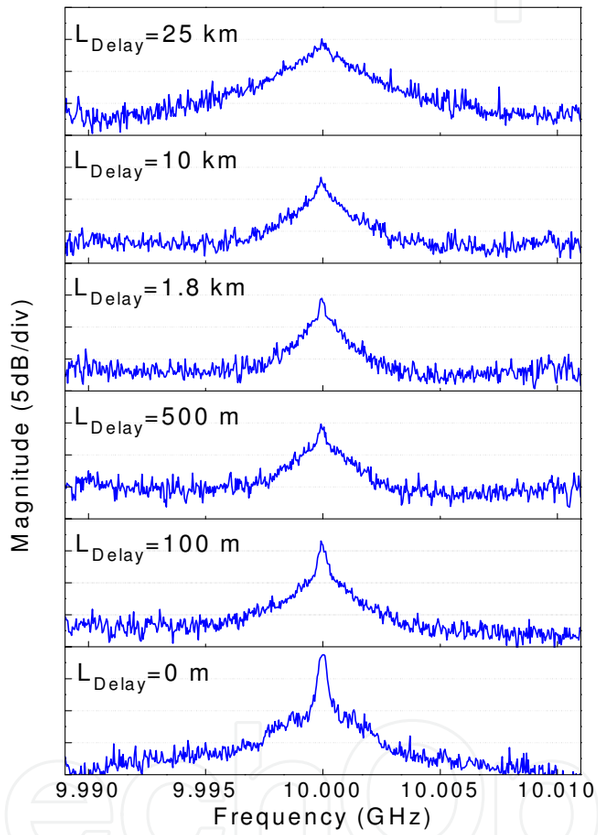

Fig. 2.17. Measured power spectra of DFB laser with fiber delay changing from 0 m to 25 km

A long delay line over coherence length of the two light beams is required to completely eliminate frequency coherence. However, long delay fiber will introduce a high insertion loss. Although an EDFA can be used to compensate the optical power level, the amplifier introduces noise and leads to a poor signal-to-noise ratio. In order to improve the previous experiment, a recirculating scheme as shown in Fig. 2.18 is proposed. In experiment, the first sidebands can be reamplified through the circulating loop. This increases the length of the delay line efficiently. It must be mentioned that this technique is not suitable for measuring linewidth since the output optical signal contains different circulation orders. The method proposed by M. Han (Chen et al., 2006; Han et al., 2005) is more suitable method for linewidth measurement.

Delay length (km)	0	0.1	0.5	1.8	10
Power ratio (dB)	7.3	4.6	3.0	2.7	0.8
10-dBlinewidth (MHz)	1.3	3.2	5.0	5.5	5.7

Table 1. Power ratio between δ-peak and Lorentzian component, and 10-dB linewidth

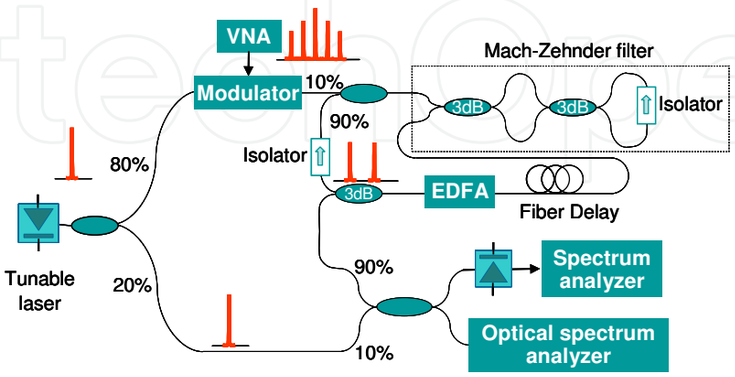

Fig. 2.18. Experimental configuration of optical self-heterodyne scheme with fiber delay loop for lineshape analysis

The peak at the modulation frequency gets wider when the recirculating scheme in Fig. 2.18 is used. For this scheme, the output optical signal comprises higher circulation-order sidebands. Thus, the beat may occur between the carrier and sidebands with a delay time in a wide time period, in which the wavelength may shift. That means that the carrier and the delayed sidebands are launched out from the lightwave source at different time. In this relatively long delay time, the optical wavelength may shift due to the instability of laser source. Consequently, broadening of the measured power spectra reveals wavelength stability of the lightwave source in the observation period. Therefore, the measured optical spectral linewidth depends on the observation time due to the instability of laser.

6. Narrow-linewidth microwave generation

Optical generation of frequency-tunable, narrow-linewidth, and stable microwave signals is desirable for many applications such as in radar, wireless communications, and satellite communication systems. Conventionally, a microwave signal can be generated in the optical domain using optical heterodyning, in which two optical waves of different wavelengths beat at a photodetector (PD). An electrical beat note is then generated at a PD, and its frequency depends on the wavelength spacing of the two optical waves (Gliese et al., 1998). This method is capable of generating microwave and millimeter wave signals. The only frequncy limit is the bandwidth of the PD. However, the beating of two optical waves from two independent optical sources would lead to a microwave with unstable frequency and high phase noise since there is no frequency coherence between them.

In the previous sections, it has been shown that the linewidth of the generated microwave signal depends only on the frequency coherence properties of the two lightwaves, not on the spectral linewidths of the individual light beams. To generate a pure microwave signal, two optical waves used for heterodyning must be highly frequency coherent(Zhu et al., 2009). This section presents two typical approaches to obtaining two frequency coherent

lightwaves. One is to make the light correlated to the light emitted in the past time from the same active region. Another way is using two correlated lightwave sources, such as two lasers with mutual injection or two monolithically integrated lasers.

6.1 Microwave generation using a self-injected DBR laser

It has been mentioned that the linewidth of the beat note between two light beams depends on the frequency coherence, not on the spectral linewidths of the two beams. Therefore, we can determine the frequency coherence of two light beams from the linewidth of their beat note.

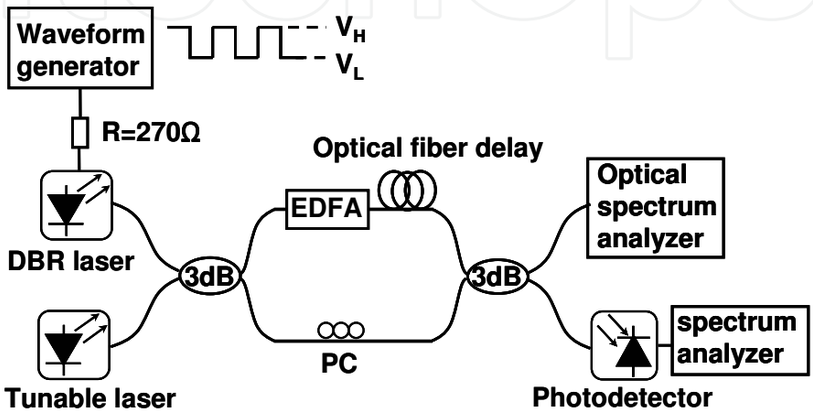

Fig. 2.19. Experimental setup

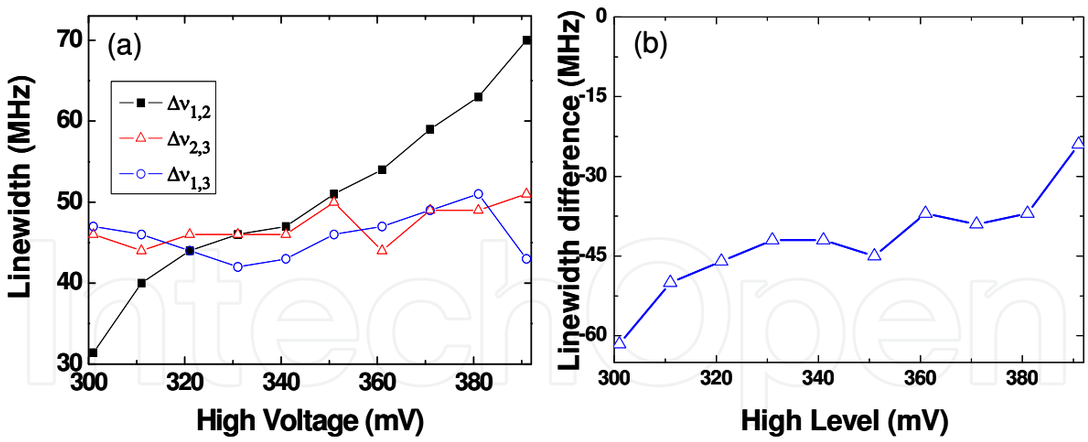

Fig. 2.20. (a) Linewidth measurement when fixing V_L at 300 mV and tuning V_H from 301 mV to 391 mV, and (b) Linewidths difference: $\Delta\nu_{1,2}$-($\Delta\nu_{2,3}$+$\Delta\nu_{1,3}$), where $\Delta\nu_{1,2}$, $\Delta\nu_{2,3}$, and $\Delta\nu_{1,3}$ are 6-dB linewidths of beat notes between λ_1 and λ_2, λ_2 and λ_3, and λ_1 and λ_3, respectively

In this system, a square-waveform voltage generated from a waveform generator (Agilient 33250A) was applied to the phase section of the DBR tunable laser. Two beams at different wavelengths λ_1 and λ_2 were generated corresponding to the high voltage V_H and low voltage V_L of the waveform, respectively. Another lightwave λ_3 from a narrow-linewidth tunable source (Agilient 8164B) was used as a reference. These lightwaves were launched

into a Mach-Zehnder interferometer and then arrived at an 18-GHz photodetector (Agilent 11982A). The spectra of their beat notes were measured by an electrical spectrum analyzer (ESA, Advantest R3182).

The optical fiber was 500 m long corresponding to a delay time of 2.5 μs, and the period of square waveform was set to be 5 μs to achieve a steady and high efficient optical heterodyne (Zhu et al., 2006). We fixed the low level V_L of the square voltage at 300 mV, and tuned the high level V_H from 301 mV to 391 mV at a step of 10 mV. In the measurement, the peak power of lightwave at λ_3 was adjusted to be equal to those of lightwaves at λ_1 and λ_2. The measured 6-dB linewidths of beat notes and the results are given in Fig. 2.20(a). $\Delta\nu_{1,2}$, $\Delta\nu_{2,3}$, and $\Delta\nu_{1,3}$ denote 6-dB linewidths of beat notes between λ_1 and λ_2, λ_2 and λ_3, and λ_1 and λ_3, respectively.

From Fig. 2.20 one can see that the measured linewidths $\Delta\nu_{1,3}$ and $\Delta\nu_{2,3}$ are between 40 and 50 MHz and do not change much in the whole tuning range. $\Delta\nu_{1,2}$ is obviously narrower than the sum of $\Delta\nu_{2,3}$ and $\Delta\nu_{1,3}$ when V_H is 301 mV and increases with the increment of V_H. Linewidth of the optical lightwave from DBR laser may broaden with the increase of phase section voltage, but in our experiment, the tuning range is rather small (~90 mV) during which the broadening effect does not that apparent as shown in Fig. 2.20 and can be ignored. Additionally, the square-wave modulation to phase section of DBR laser may cause jitter of the emitted lightwaves and thus affect the linewidth measurement. However, in this experiment, we only care about the comparison between the linewidth of the beat note $\Delta\nu_{1,2}$ and the sum of linewidths of the two lightwaves ($\Delta\nu_1+\Delta\nu_2$), not the absolute linewidth value. Thus, we plotted the difference between them in Fig. 2.20(b). The jitter can be eliminated after making the subtraction. Since linewidth of the lightwave λ_3 from the narrow-linewidth tunable laser is narrower than 100 kHz, $\Delta\nu_3$ can be neglected. The difference can be written as,

$$\Delta\nu_{1,2}-(\Delta\nu_{1,3}+\Delta\nu_{2,3})\approx\Delta\nu_{1,2}-(\Delta\nu_1+\Delta\nu_2) \tag{16}$$

As shown in Fig. 2.20(b), in the tuning range, the linewidth of beat note between the ligtwaves at λ_1 and λ_2 is apparently narrower than the sum of that of the two lightwaves. The difference between them is diminishing as the increase of V_H. Although the curve is not smooth due to the accumulated measurement error, the trend is obvious.

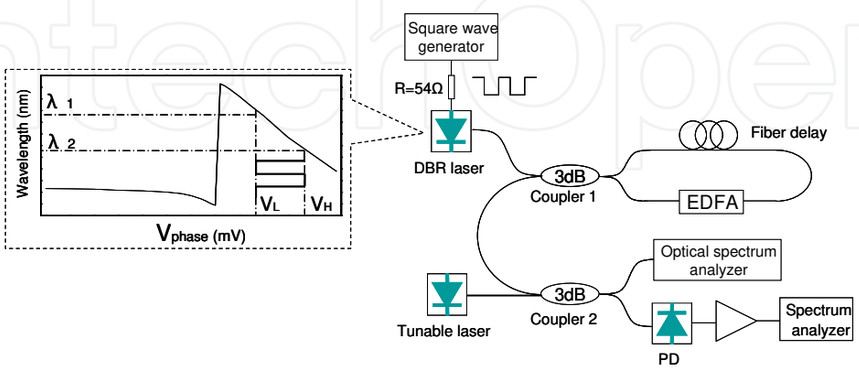

Fig. 2.21. Delayed optical self-injection system

These results reveal that the two lightwaves at λ_1 and λ_2 from the same active region of DBR laser are partially frequency coherent when voltage difference between V_H and V_L is smaller

(i.e., the wavelengths of the two lightwaves are close), and the coherence of the two light beams becomes weaker as the increase of the amplitude of the square-waveform voltage.
The frequency coherence between the two lightwaves is weak because they are generated asynchronously. By a method of delayed optical self-injection, the lightwave λ_1 and λ_2 can be generated synchronously. The experimental setup of delayed optical self-injection is shown in Fig. 2.21.
In this system, the laser source is a sampled-grating distributed Bragg reflector (SG-DBR) laser without isolator. A square-wave voltage is applied to the phase section of the laser source. As shown in the insert figure, two lightwaves at different wavelengths λ_1 and λ_2 are generated alternately corresponding to the higher voltage V_H and the lower voltage V_L. After a fiber delay the lightwaves are injected back to the laser. The delay time is exactly equal to the half period of the square-wave voltage. Thus, when the laser oscillated at λ_1 (or λ_2), the injected lightwave is at λ_2 (or λ_1). Then the DBR laser can generate two lightwaves at both λ_1 and λ_2 simultaneously.

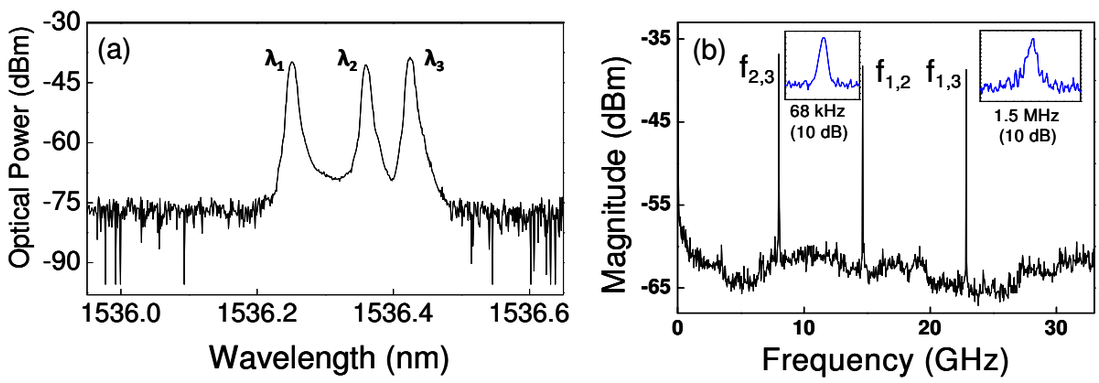

Fig. 2.22. (a)Optical spectra of lightwaves and (b) electrical spectra of their beat notes, where $f_{1,2}$, $f_{2,3}$ and $f_{1,3}$ denote the beat notes generated by the lightwaves λ_1 and λ_2, λ_2 and λ_3, and λ_1 and λ_3 respectively

The optical spectra of the lightwaves are shown in Fig. 2.22(a). The electrical spectra of their beat notes are described in Fig. 2.22(b). $f_{1,2}$, $f_{2,3}$ and $f_{1,3}$ denote the beat notes generated by the lightwaves λ_1 and λ_2, λ_2 and λ_3, and λ_1 and λ_3 respectively. The insert figures are the refined electrical spectra of $f_{1,2}$ and $f_{1,3}$. The 10-dB linewidths of beat notes $f_{1,2}$ and $f_{1,3}$ are 68 kHz and 1.5 MHz, respectively, which are much narrower than that of the lightwaves. There are two reasons for the linewidth reduction. For one thing, the fiber ring used for the optical feedback configures an external cavity. The cavity narrows the linewidth of lightwaves and suppresses the noise of the laser. For another, by optical self-injection, the two lightwaves λ_1 and λ_2 are generated synchronously. The frequency coherence between the two lightwaves is enhanced, which further narrows the linewidths of the beat notes.
The method of the delayed optical self-injection makes the active region oscillate at two different wavelength simultaneously, which strengthens the frequency coherence between the two lightwaves. This method provides us an effective way to generate the microwave signals with narrow linewidth and low phase noise.

6.2 Monolithically integrated microwave source

Fig. 2.23 shows the experimental setup for microwave signal generation based on an EML, which emits one light beam. Another light beam from a narrow-linewidth tunable laser is

injected into the electro-absorption modulator (EAM) through an optical circulator. These two beams mixed in the modulator. It has been observed that a reversely biased EAM can be utilized as high-frequency pohotodetector to generate beat signal (Wood et al., 1986; Westbrook et al., 1996). The frequency of the generated signal exactly depends on the wavelength difference, and the power can be expressed as:

$$P_{\text{Microwave}} = \frac{1}{4}(mP_{\text{opt}}R)^2 R_{\text{d}} \tag{17}$$

where m is the modulation depth, P_{opt} is the optical power coupled into EAM, R is the DC responsibility, and R_d is the load impedance.

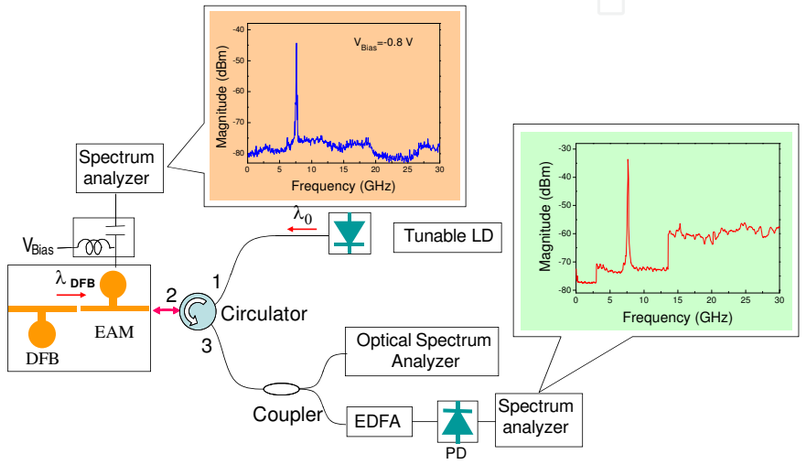

Fig. 2.23. Microwave generation by EML subject to optical injection

As shown in Fig. 2.23, the EAM is biased through a bias Tee and the generated microwave signal from the EAM was measured by an ESA. The output from port 3 of the optical circulator consists of the lightwaves from the DFB laser and the tunable laser. The mixed lightwaves are split into two waves by a coupler. One of them is launched into an optical spectrum analyzer (OSA). Another is received by a high-speed photodetector and the electrical spectra are measured by another ESA. In this way, the spectrum of the microwave signals generated in both the high-speed photodetector and the EAM can be measured simultaneously, as shown in the insets of Fig. 2.23. It has been shown that the frequency of the microwave generated in the EAM can be tuned when the wavelength of the DFB laser is fixed and the wavelength of the narrow-linewidth tunable laser is changed. On the other hand, the wavelength of the DFB laser can be shifted by adjusting the bias voltage of the EAM due to adiabatic chirp. When the isolation resistance between the EAM and the integrated DFB laser is not large enough, the laser working current will vary with the reverse bias voltage. This results in the laser wavelength shift, and can be used for fine tuning of the frequency of the generated microwave signal.

Based on the above work, a tunable monolithic microwave source is proposed (Zhu et al., 2009). The schematic diagram of the chip and the experiment setup is shown in Fig. 2.24. The structures of the modulator and lasers are similar to those of the devices shown in Fig. 2.23. In this scheme, the wavelengths of the two DFB lasers can be tuned by adjusting their bias currents respectively. The lightwaves emitted from both DFB lasers are injected into the

EAM and mixed with each other to generate a microwave signal. A lensed fiber is used to monitor the change of the optical wavelength.

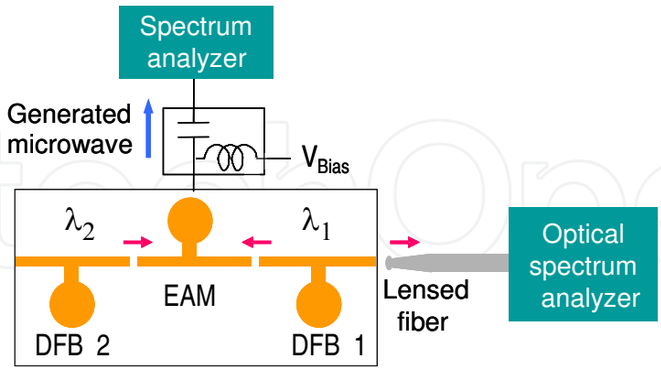

Fig. 2.24. Microwave signal generation using an EAM integrated in between two DFB lasers

Fig. 2.25 shows the output optical and electrical spectra. From Fig. 2.25(a), it can be seen that the four-wave mixing still exists when the optical wavelength difference is over 30 GHz due to strong optical coupling between the two lasers. In Fig. 2.25(b), there is a sharp peak at the beat frequency with a signal to noise ratio of 24-dB. The frequency of the generated microwave signal can be tuned by changing the bias currents of the DFB lasers. Here, the modulator in this device has three functions:

1. Generate microwave signal.
2. Tune the frequency of the generated microwave.
3. Control the intensity of the generated microwave.

The results show that an EAM integrated in between two DFB lasers can be used as a monolithic integrated microwave source.

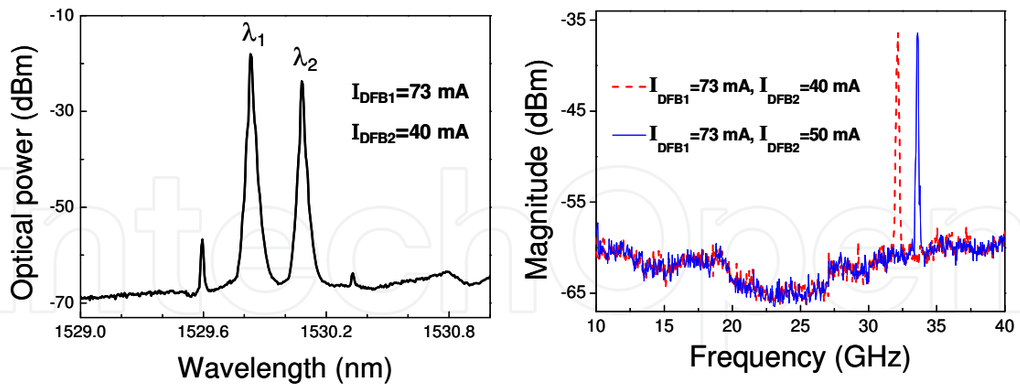

Fig. 2.25. (a) Optical spectrum and (b) corresponding electrical spectrum (dashed line). The electrical spectrum after adjusting the bias current of the DFB laser 2 is also included

7. References

A. A. Michelson (1927). *Studies in Optics,* University of Chicago Press, Chicago

Born, M. & Wolf, E. (1999). *Principles of Optics (7th ed),* Cambridge University Press, ISBN 0 521 642221, New York

Chan, E. H. W. (2007). Coherence-free optical delay line signal processor. *Electron. Lett.,* Vol. 43, No. 17, (Aug. 2007) 947-948, ISSN 0013-5194.

Chen, X. P.; Han, M.; Zhu, Y. Z.; Dong, B. & Wang, A. B. (2006). Implementation of a loss-compensated recirculating delayed self-heterodyne interferometer for ultranarrow laser linewidth measurement. *Appl. Opt.*, Vol. 45, No.29, (Oct. 2006) 7712-7717, ISSN 0003-6935.

Dawson, J. W.; Park, N. & Vahala, K. J. (1992). An improved delayed self-heteodyne interferometer for linewidth measurements. *IEEE Photon. Technol. Lett.*, Vol. 4, No. 9, (Sept. 1992) 1063-1066, ISSN 1041-1135.

Devaux, F.; Sorel, Y. & Kerdiles, J. F. (1993). Simple measurement of fiber dispersion and of chirp parameter of intensity modulated light emitter. J. Lightwave Technol., Vol. 11, No. 12, (Dec. 1993) 1937-1940, ISSN : 0733-8724.

Diitchburn, R. W. (1963). *Light*, Blackie & Son Ltd., Glasgow.

Eichen, E. & Silletti, A. (1987). Bandwidth measurements of ultrahigh-frequency optical detectors using the interferometric FM sideband technique. *J. Lightwave Technol.,* Vol. 5, pp. 1377-1381

Gliese, U.; Nielsen, T. N.; Nørskov, S. & Stubkjær, K. E. (2005). Narrow linewidth fiber laser for 100-km optical frequency domain reflectometry. *IEEE Photon. Technol. Lett.*, Vol. 17, No. 9, (Sept. 2005) 1827-1829, ISSN 1041-1135.

Geng, J.; Spiegelberg, C. & Jiang, S. (2005). Narrow linewidth fiber laser for 100-km optical frequency domain reflectometry. *IEEE Photon. Technol. Lett.*, Vol. 17, No. 9, (Sept. 2005) 1827-1829, ISSN 1041-1135.

Han, M. & Wang, A. (2005). Analysis of a loss-compensated recirculating delayed self-heterodyne interferometer for laser linewidth measurement. *Appl. Phys. B*, Vol. 81, (Jul. 2005) 53-58, ISSN 0946-2171.

Henry, C. H. (1982) Theory of the linewidth of semiconductor lasers. *IEEE J.Quantum Electron.*, Vol. 18, No. 2, (May 2009) 259-264, ISSN 0018-9197.

Ke, J.; Zhu, N.; Zhang, H.; Man, J.; Zhao, L.; Chen, W.; Wang, X.; Liu, Y.; Yuan, H.; Xie, L. & Wang, W. (2009). Frequency and Temporal Coherence Properties of Distributed Bragg Reflector Laser. *Microwave Opt. Technol. Lett.*, Vol. 52, No. 4, (Aprial, 2010)822-825, ISSN 0895-2477

Ludvigsen, H.; Tossavainen, M. & Kaivola, M. (1998). Laser linewidth measurements using self-homodyne detection with short delay. *Opt. Commun.,* Vol. 155, No. 5, (Oct. 1998) 180-186, ISSN 0030-4018.

Mandel, L. & Wolf, E. (1965). Coherence Properties of Optical Fields, *Rev. Mod. Phys.,* Vol. 37, No. 2, pp. 231-287

Mandel, L. & Wolf, E. (1976). Spectral coherence and the concept of cross-spectral purity. *J. Opt. Soc. Am.*, Vol. 66, No. 6, (Jun. 1976) pp. 529-535

Mandel, L. & Wolf, E. (1995) *Optical Coherence and Quantum Optics*, Cambridge University.

Mathieu, J. P. (1975). *Optics*, Oxford, 0080171575, New York.

Richter, L. E.; Mandelberg, H. I.; Kruger, M. S. & Mcgerath, P. A. (1986). Linewidth determination from self-heterodyne measurements with subcoherence delay times. *IEEE J. Quantum Electron.*, Vol. QE-22, No. 11, (Nov. 1986) 2070-2074, ISSN 0018-9197.

Ryabukho, V.; Lyakin, D. & Lobachev, M. (2005). Longitudinal pure spatial coherence of a light field with wide frequency and angular spectra. *Opt. Lett.*, Vol. 30, No. 3, (Feb. 2005) 224-226, ISSN 0146-9592.

Sato, K. (2001). 100 GHz optical pulse generation using Fabry-Perot laser under continuous wave operation. *Electron. Lett.,* Vol. 37, No. 12, (June, 2001) 763-764, ISSN 0013-5194

Signoret, P.; Marin, F.; Viciani, S.; Belleville, G.; Myara, M. & Tourrenc, J. P. (2001). 3.6 MHz linewidth 1.55μm monomode vertical-cavity surface-emitting laser. *IEEE Photon. Technol. Lett.*, Vol. 13, No. 4, (Apr. 2001) 269-271, ISSN 1041-1135.

Signoret, P.; Myara, M.; Tourrenc, J. –P.; Orsal, B.; Monier, M. –H.; Jacquet, J.; Leboudec, P. & Marin, F. (2004). Bragg section effects on linewidth and lineshape in 1.55-μm DBR tunable laser diodes. *IEEE Photon. Technol. Lett.*, Vol. 16, No. 6, (Jun. 2004) 1429-1431, ISSN 1041-1135.

Sun, C.; Zhu, J.; Liu, Y. & Yu P. (1996). Dual-function electroabsorption waveguide modulator/detector for optoelectronic transceiver applications. *IEEE Photon. Technol. Lett.*, Vol. 8, No.11, (November, 1996)1540-1542, ISSN 1041-1135

Wheeler, C. R.; Ramsier, R. D. &Henriksen, P. N. (2003). An investigation of the temporal coherence length of ligh. *Eur. J. Phys.*, Vol. 24, No. 4, (2003) 443-450, ISSN 0143-0807.

Wood, T.; Carr, E.; Kasper, B.; Linke, R. & Burrus, C. (1986). Bidirectional fibre-optical transmission using a multiple-quantum-well (MQW) modulator/detector. *Electron. Lett.*, Vol. 22, No. 10, (March, 1986)528-529, ISSN 0013-5194

Yariv, A. (1997). *Optical Electronics in Modern Communications,* Oxford University Press, ISBN-13: 9780195106268, New York

Zhang, H.; Zhu, N.; Man, J.; Ke, J.; Zhang, B.; Han, W.; Chen, W.; Wang, X.; Xie, L.; Zhao, L. & Wang, W. (2009). Narrow-linewidth microwave generation using a self-injected DBR laser diode. *IEEE Photon. Technol. Lett.*, Vol.21, No.15, (August, 2009)1045-1047, ISSN 1041-1135

Zhu, N. H.; Wen, J. M.; Chen, W. & Xie, L. (2007). Hyperfine spectral structure of semiconductor lasers. *Physical Review A*, Vol. 76, (Dec. 2007) 063821, ISSN 1050-2947.

Zhu, N. H.; Li, W.; Wang, L. X.; Chen. S. F. & Ke, J. H. (2009). Study on frequency coherence properties of light beams. *IEEE J. Quantum Electron.*, Vol. 45, No. 5, (May. 2009) 514-522, ISSN 0018-9197.

Zhu, N. H.; Man, J. W.; Zhang, H. G. & Ke, J. H. et al (2010). Lineshape analysis of the beat note between optical carrier and delayed sidebands. *IEEE J. Quantum Electron.*, Vol. 46, No. 3, (Mar. 2010) 347-353, ISSN 0018-9197.

Zhu, N. H.; Wen, J. M.; Song, H. P.; Zhang, S. J. & Xie, L. (2006). Measurement of small-signal and large-signal responses of packaged laser modules at high temperature. *Opt. Quantum Electron.,* Vol. 38, (December, 2006) 1245-1257, ISSN 0306-8919

Zhu, N.; Zhang, H.; Man, J.; Zhu, H.; Ke, J.; Liu, Y.; Wang, X.; Yuan, H.; Xie, L. & Wang, W. (2009). Microwave generation in an electro-absorption modulator integrated with a DFB laser subject to optical injection. *Optical Express*, Vol. 17, No. 24, (November, 2009) 22114-22123, ISSN 1094-4087

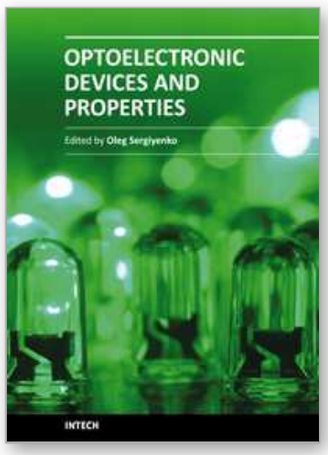

Optoelectronic Devices and Properties

Edited by Prof. Oleg Sergiyenko

ISBN 978-953-307-204-3
Hard cover, 660 pages
Publisher InTech
Published online 19, April, 2011
Published in print edition April, 2011

Optoelectronic devices impact many areas of society, from simple household appliances and multimedia systems to communications, computing, spatial scanning, optical monitoring, 3D measurements and medical instruments. This is the most complete book about optoelectromechanic systems and semiconductor optoelectronic devices; it provides an accessible, well-organized overview of optoelectronic devices and properties that emphasizes basic principles.

INTECH
open science | open minds

InTech Europe
University Campus STeP Ri
Slavka Krautzeka 83/A
51000 Rijeka, Croatia
Phone: +385 (51) 770 447
Fax: +385 (51) 686 166
www.intechopen.com

InTech China
Unit 405, Office Block, Hotel Equatorial Shanghai
No.65, Yan An Road (West), Shanghai, 200040, China
中国上海市延安西路65号上海国际贵都大饭店办公楼405单元
Phone: +86-21-62489820
Fax: +86-21-62489821

IntechOpen